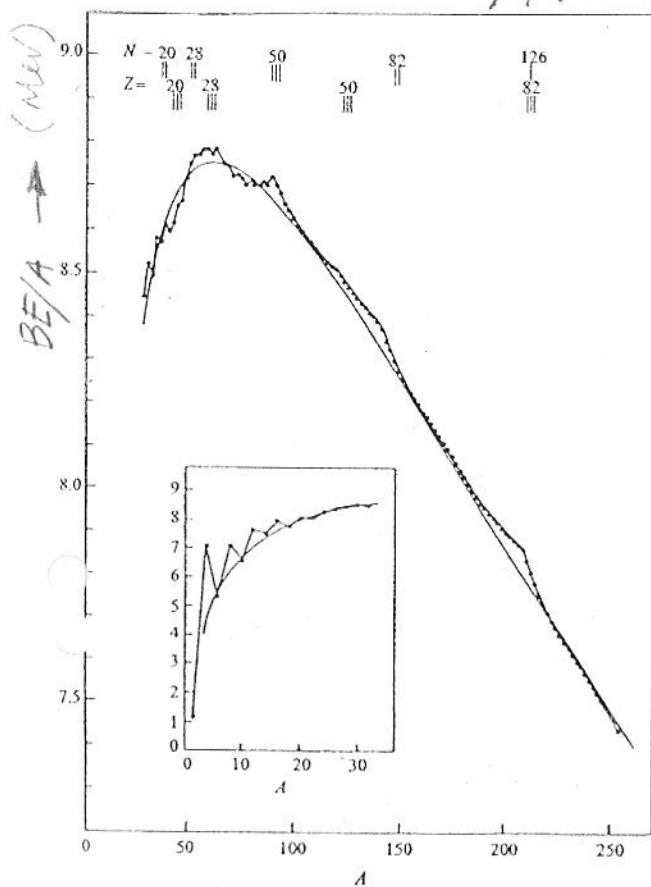


- *Eveptia orobrotus* : BE uai BE/A

Fig.

Vouagovio : BE/A



(Staggering)

δ_N o-e staggering in S_N

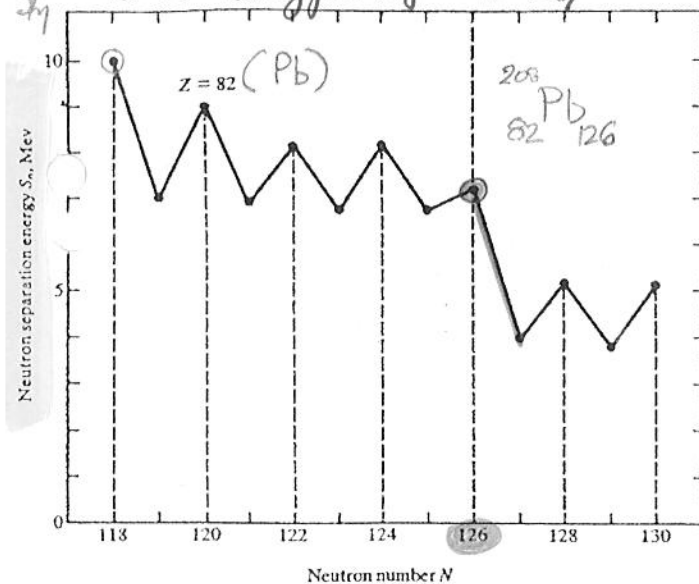


Figure 2.2 Neutron separation energy for the lead isotopes.

$$S_N = BE(A, Z) - BE(A-1, Z)$$

Kontakos Thymvris
σταθεόμας

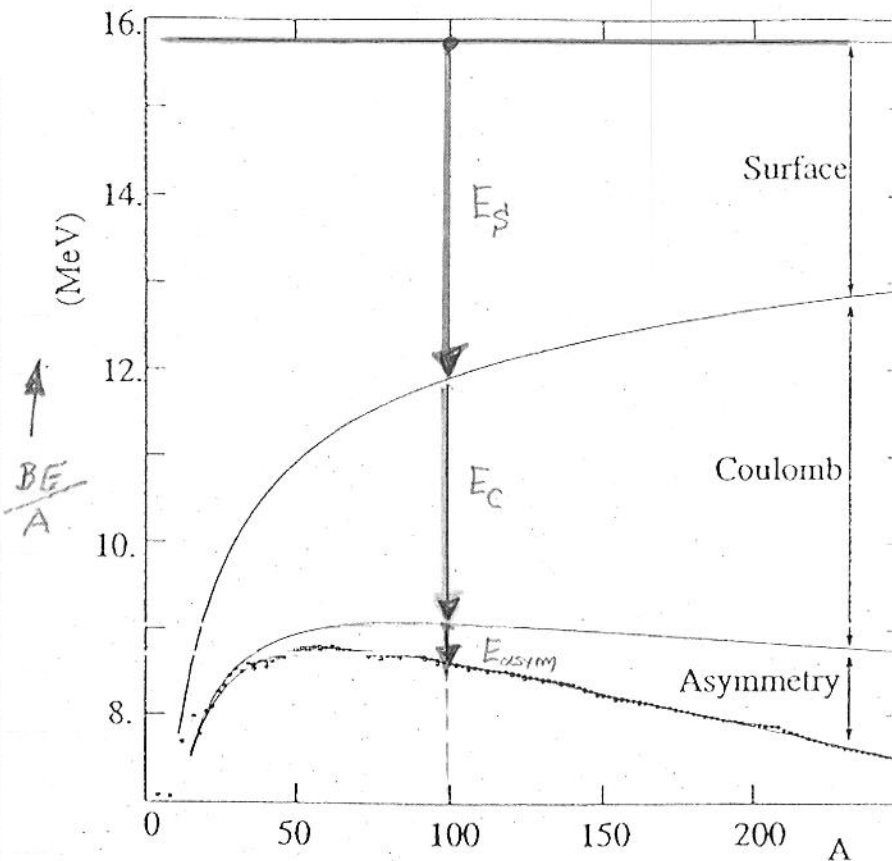


Fig. 2.5. The observed binding energies as a function of A and the prediction of the mass formula (2.13). For each value of A , the most bound value of Z used corresponding to $Z = A/2$ for light nuclei but $Z < A/2$ for heavy nuclei. Only even-odd combinations of A and Z are considered where the pairing term in the mass formula vanishes. Contributions to the binding energy per nucleon of the various terms in the mass formula are shown.

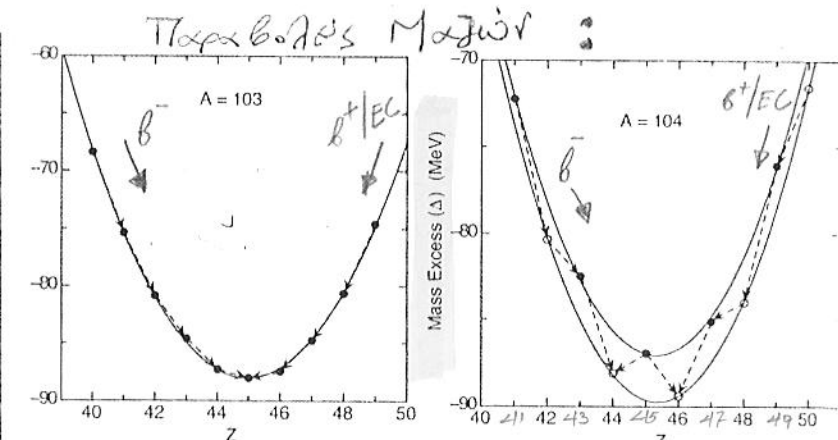
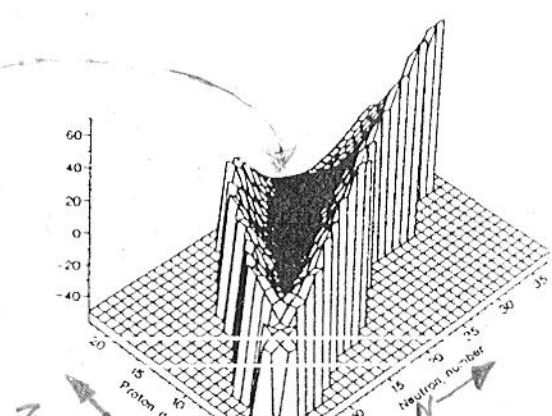


Fig. 5.4 Experimental mass excesses (MeV) for the isobars of $A=103$ and $A=104$. The curves shown are fits with the semi-empirical mass formula.

$$\Delta = [M-A]c^2$$



Κατκροφί^η
 Πλινθόμελ
 φοετίου
 (Πρωτογενίων)
 [Περιπλάκα]

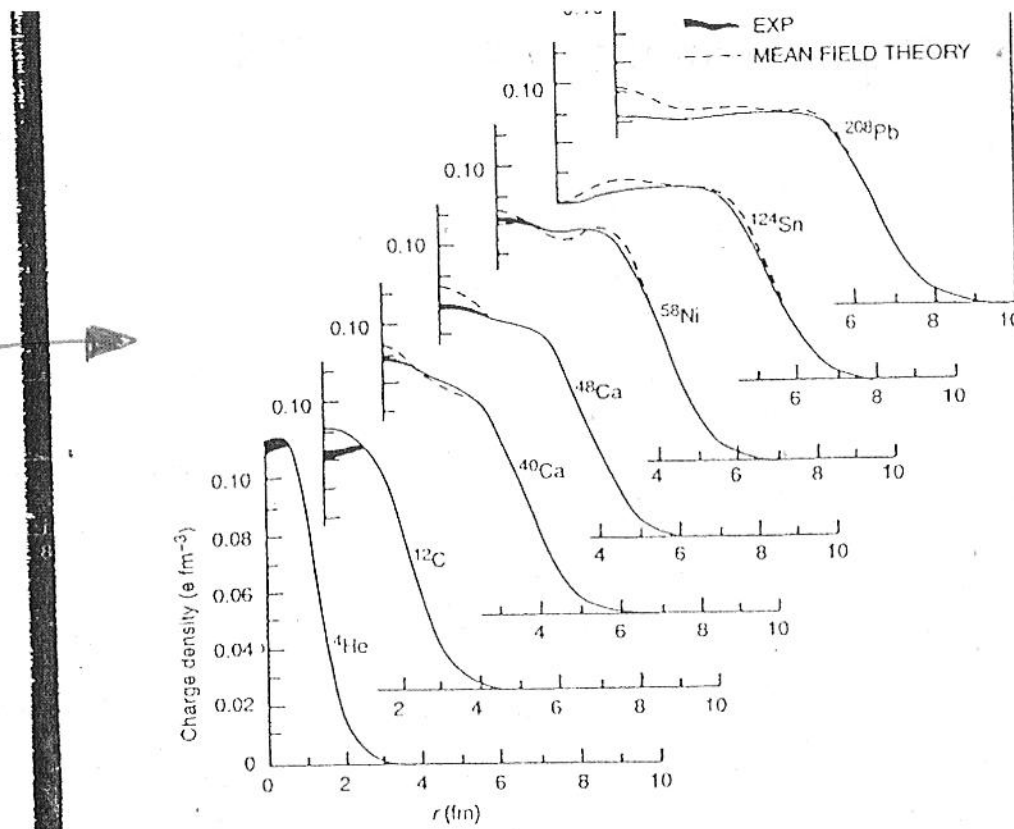


Figure 2.11 Nuclear ground-state charge distributions as measured for a sample of nuclei throughout the periodic table from B. Frois, Proc. Int. Conf. Nucl. Phys., Florence, 1983, eds. P. Blasi and R.A. Ricci (Tipografia Compositori Bologna) Vol. 2, p. 221.'

$^{208}\text{Pb}_{82,126}$

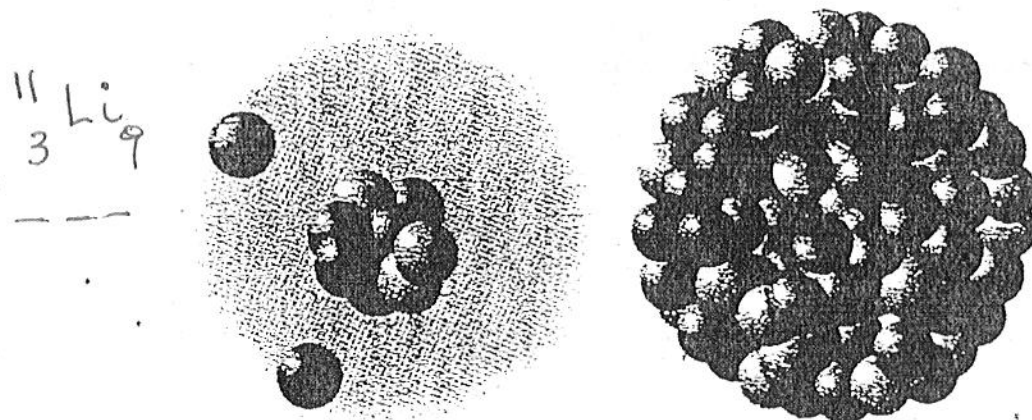


Figure 2.12 Schematic representation of the relative sizes of the halo nucleus ^{11}Li and ^{208}Pb . (Figure also appears in color figure section.)

$$n-l = 2(N-1)$$

(oscillator quantum #)

(οικεῖος αριθμός
Ενός αγωγού πέτρας τροχαντού ℓ)

Ενέργεια και διάγραμμα του Προτύπου

στιλάδειν

Ενέργεια επίπεδα 1
150 τρόπου γρήγορου
ταξιτωνού

spin-orbit
Splitting

Αριθμός
νούντερινι

Συνολικός
Αριθμός
Νούντερινι

Συνολικός
αριθμός
Νούντερινι

168 (56)

112 (42)

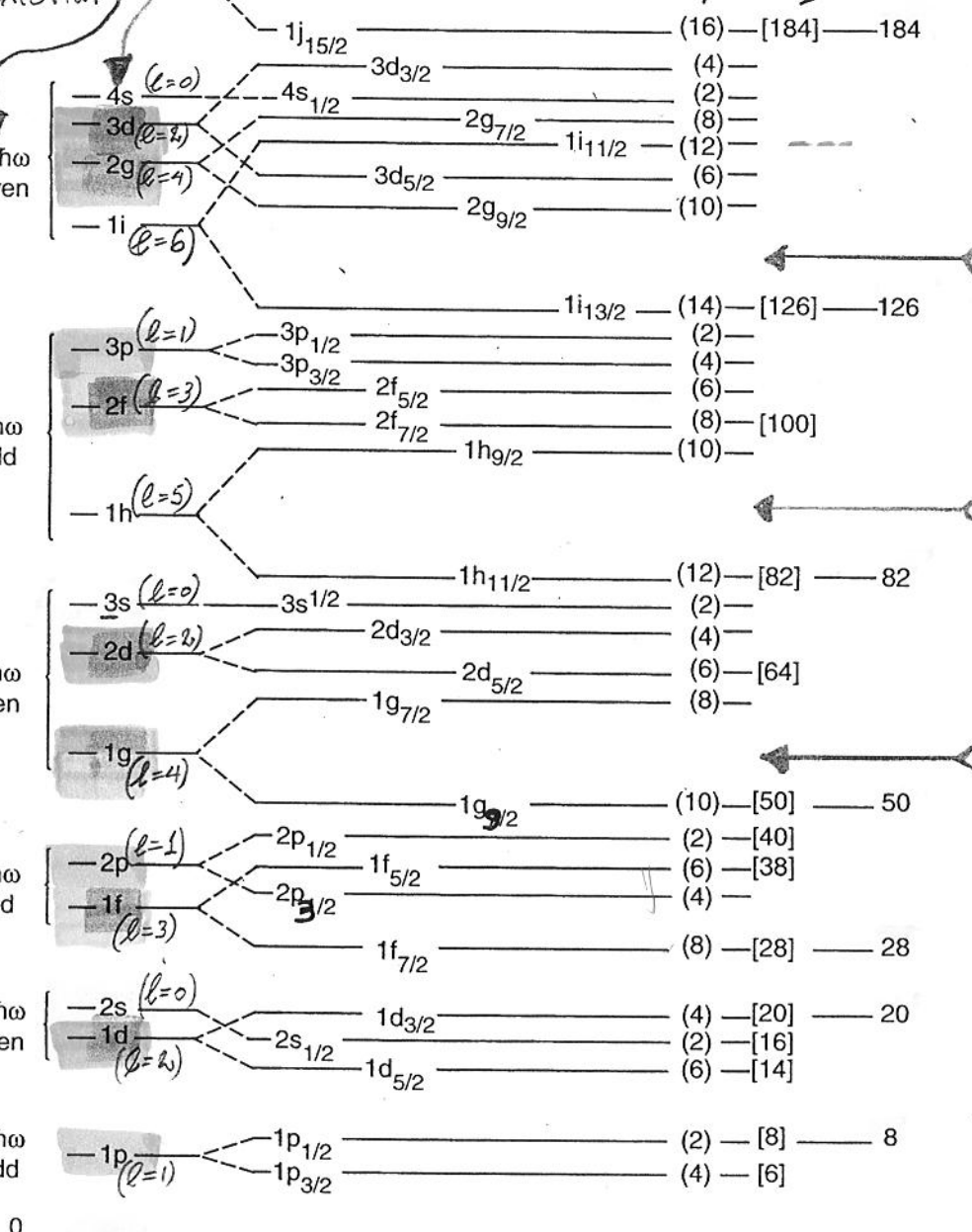
70 (30)

40 (20)

20 (12)

8 (6)

2 (2)



ΜΑΓΙΚΟΙ
ΑΡΙΘΜΟΙ
"Jp - shell"

"Sd - shell"
 $A = 17-40$

"P - shell"
 $A = 5-16$

"S - shell"

Figure 6.3 Energy level pattern and spectroscopic labeling of states from the schematic shell model. The angular momentum coupling is indicated at the left side and the numbers of nucleons needed to fill each orbital and each shell are shown on the right side. From M. G. Mayer and J. H. D. Jensen, Elementary Theory of Nuclear Shell Structure, Wiley, New York, 1955.

[W. Loveland Book p. 143]

| $\ell =$ | 0 | 1 | 2 | 3 | 4 | 5 | 6 | 7 |
|----------|---|---|---|---|---|----|----|----|
| S | P | d | f | g | h | i | j | |
| 2ℓ+1 | 1 | 3 | 5 | 7 | 9 | 11 | 13 | 15 |
| L | | | | | | | | |

$n = 0, 1, 2, 3, 4, 5, 6, 7$

$n = \text{even} \Rightarrow \ell = 0, 2, 4, 6$

$n = \text{odd} \Rightarrow \ell = 1, 3, 5, 7, 9$

$$\Delta \left(\frac{B/A}{A} \right) = \left(\frac{B/A}{A} \right)_{\text{exp}} - \left(\frac{B/A}{A} \right)_{\text{LDM}}$$

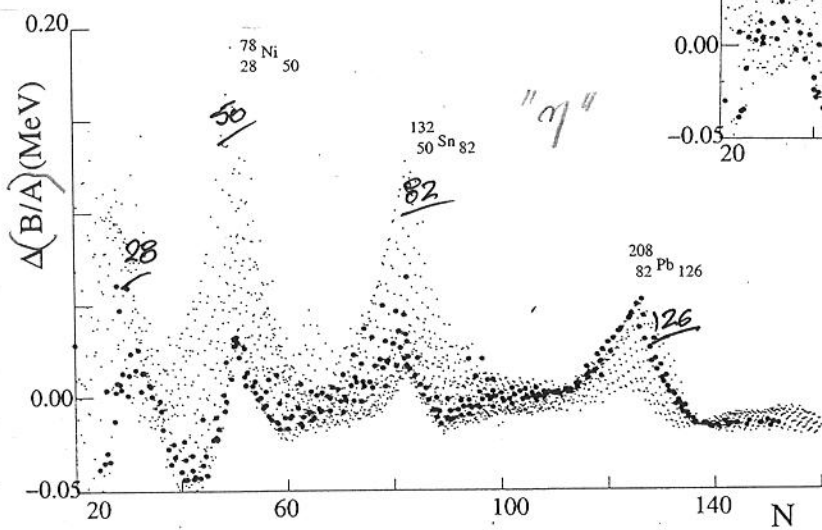
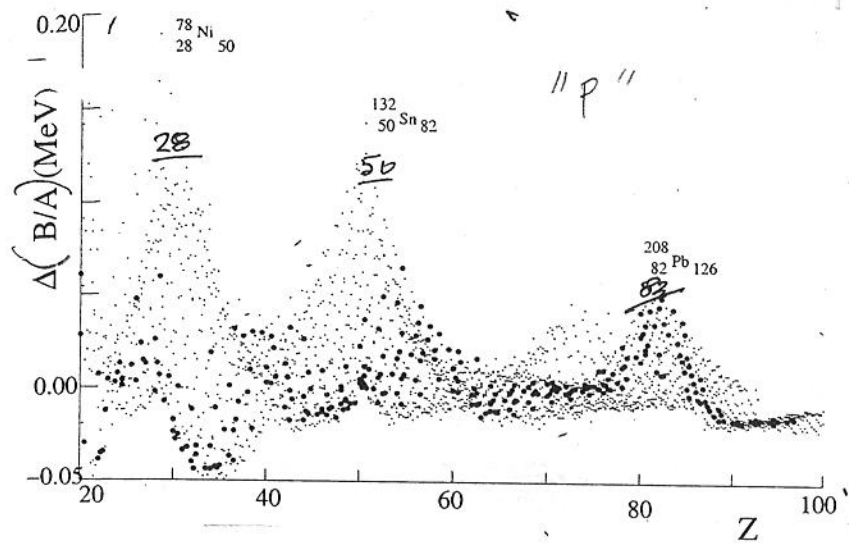


Fig. 2.8. Difference in MeV between the measured value of B/A and the value calculated with the empirical mass formula as a function of the number of protons Z (top) and of the number of neutrons N (bottom). The large dots are for β -stable nuclei. One can see maxima for the magic numbers $Z, N = 20, 28, 50, 82$, and 126 . The largest excesses are for the doubly magic nuclides as indicated.



EXPERIMENTAL EVIDENCE FOR MAGIC NUMBERS

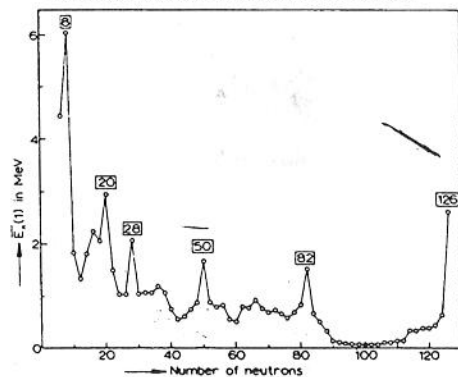
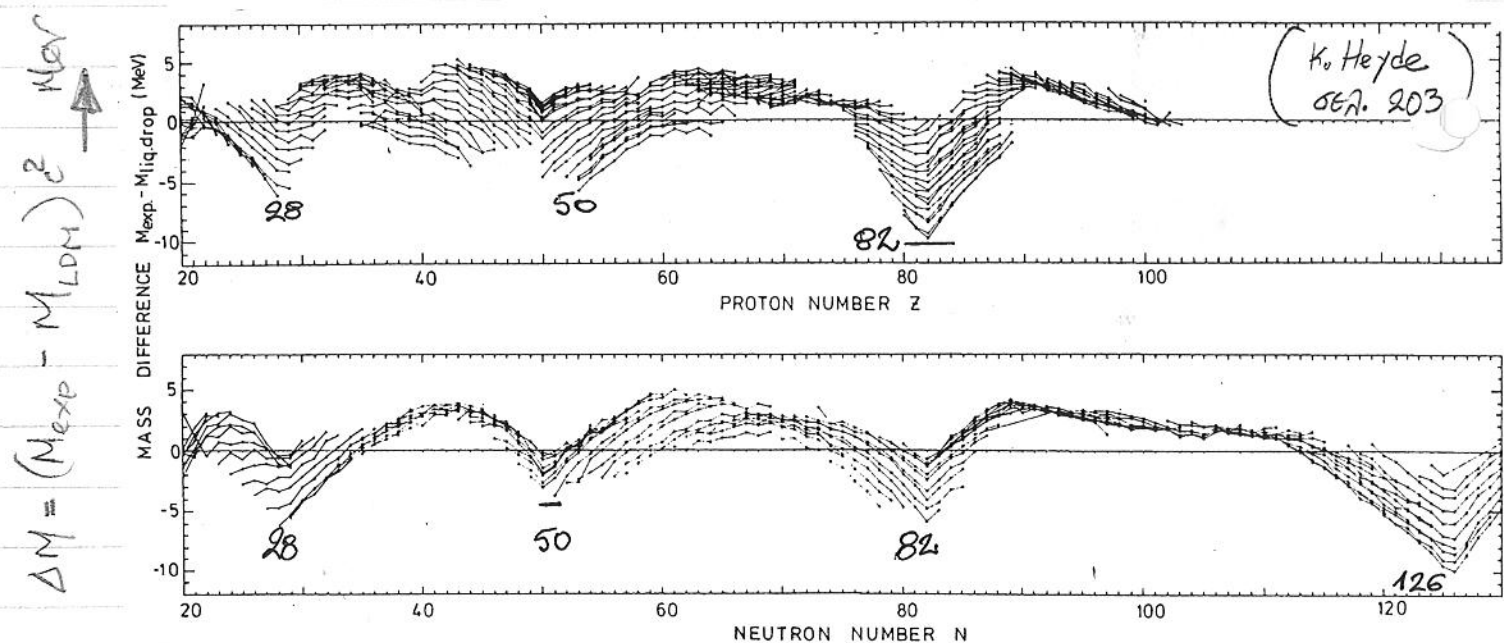


Figure 9.4. The occurrence of magic numbers as demonstrated by the average excitation energy of the first excited state in doubly-even nuclei, as a function of neutron number N (taken from Brussaard and Glaudemans 1977).



• LDM : Liquid Drop Model (Eisberg Bethe-Weizsäcker)

Figure 7.13. Nuclear (liquid drop) masses and the deviations with respect to the nuclear data and this, as a function of proton and neutron number. The shell closure effects are shown most dramatically (adapted from Myers 1966).